AIAA JOURNAL
Vol. 56, No. 3, March 2018

Reliability Estimation Using Markov Chain Monte Carlo–Based Tail Modeling

Gamze Bayrak* and Erdem Acar†
TOBB University of Economics and Technology, 06560 Ankara, Turkey

DOI: 10.2514/1.J055947

Tail modeling is an efficient method used in reliability estimation of highly safe structures. Classical tail modeling is based on performing limit-state function evaluations through a sampling scheme, selecting a threshold value to specify the tail part of the cumulative distribution function, fitting a proper model to the tail part, and estimating the reliability. In this approach, limit-state function calculations that do not belong to the tail part are mostly discarded, and so majority of limit-state evaluations are wasted. In this paper, Markov chain Monte Carlo method with Metropolis–Hastings algorithm is used to draw samples from the tail part only so that a more accurate reliability index prediction is achieved. A commonly used proposal distribution formula is modified by using a scale parameter. The optimal value of this scale parameter is obtained for various numerical example problems with a varying number of random variables, and an approximate relationship is obtained between the optimal value of the scale parameter and the number of random variables. The approximate relationship is tested on the reliability prediction of a horizontal axis wind turbine and observed to work well. It is also found that the proposed approach is more accurate than the classical tail modeling when the number of variables is less than or equal to four. For a larger number of random variables, none of the two approaches are found to be superior to another.

Nomenclature

F_t	=	threshold value of the cumulative distribution function of the limit-state function to define the tail part
k	=	proposal distribution scale parameter
k^*	=	optimal value of the proposal distribution scale parameter
N	=	number of samples in the tail part
N_t	=	total number of samples
y_t	=	threshold value of the limit-state function to define the tail part

I. Introduction

THE limit-state function (LSF) of a structural system is usually evaluated through performing computationally expensive finite element analyses. The simulation techniques such as Monte Carlo method [1] or its advanced variants (e.g., importance sampling [2], adaptive importance sampling [3], directional simulation [4]) require a large number of LSF evaluations compared with analytical methods; hence, they are not suitable for reliability prediction of highly safe structural systems. Alternatively, the analytical methods such as first-order reliability method (FORM) or second-order reliability method (SORM) are computationally efficient, but their accuracy diminishes as the LSF becomes nonlinear. To overcome the drawbacks of these traditional methods, the techniques based on tail modeling have been successfully used for reliability estimation at high reliability levels [5–8]. Boos [5] and Hasofer [6] showed that the order statistics can be used to estimate small probabilities of failure associated with the structural systems. Caers and Maes [7] proposed to use a finite sample mean square error for estimating the tail characteristics. Ramu et al. [8] proposed the multiple tail median technique that is based on the use of the median value of five different tail model predictions and applied this method for reliability prediction of a composite laminate that operates in cryogenic temperatures.

Reliability estimation using tail modeling is based on approximating the tail of the cumulative distribution function (CDF) of the LSF. Classical tail modeling (CTM) methods are based on the following procedure: First a set of LSF evaluations through a sampling scheme (e.g., Monte Carlo simulations [MCS]) is performed. Then, a proper threshold value of the CDF is selected that specifies the tail part (e.g., 90% threshold). Finally, a proper tail model is fitted to the tail part (i.e., the portion above the threshold value). In this procedure, only the tail part of the LSF evaluations is used in finding the parameters of the tail model, whereas the rest of the data are discarded. That is, the efforts spent for performing LSF evaluations that do not belong to the tail part are mostly wasted.

To reduce the amount of unused data, more efficient techniques based on steering the sampling points toward the tail region by using surrogate models [9,10] and convex hull [11] have been proposed. Acar [9] guided the limit-state evaluations through a procedure based on approximating the LSF and calculating the statistical moments of the LSF using the univariate dimension reduction method [12] along with distribution fitting using extended generalized lambda distributions [13]. Support vector machines are also used to guide the sampling points [10]. Ramu and Krishna [11] used an adaptive convex hull strategy for efficient tail modeling. They performed a relatively small number of limit-state evaluations, identified the cluster of tail samples, and wrapped a convex hull around it. The hull is progressively updated with limited additional limit-state evaluations around the boundary of initial hull. Finally, tail modeling is performed using the converged hull. It is found in those studies that if the LSF is highly nonlinear and the problem dimension is high, the construction of an accurate surrogate model or an accurate and converged hull becomes difficult, and so the efficiency of these techniques diminishes.

In this paper, Markov chain Monte Carlo (MCMC) method with Metropolis–Hastings (MH) algorithm is blended with CTM to increase the efficiency of the CTM. A commonly used proposal distribution formula is modified by using a scale parameter. The optimal value of this scale parameter is obtained for various numerical example problems with a varying number of random variables, and an approximate relationship is obtained between the optimal value of the scale parameter and the number of random variables. The proposed method is applied to numerical example problems as well as reliability prediction of a horizontal axis wind turbine, and the accuracy of the proposed method is compared with that of the CTM.

Presented as Paper 2016-4412 at the 17th AIAA/ISSMO Multidisciplinary Analysis and Optimization Conference, Washington, D.C., 13–17 June 2016; received 22 December 2016; revision received 8 September 2017; accepted for publication 14 September 2017; published online 16 October 2017.

*Graduate Research Assistant, Department of Mechanical Engineering, Söğütözü.

†Associate Professor, Department of Mechanical Engineering, Söğütözü. Associate Fellow AIAA.

This paper is organized as follows: A brief overview of the CTM and MCMC methods is provided in Sec. II. The proposed method is explained in Sec. III, and applied to numerical example problems as well as reliability prediction of a horizontal axis wind turbine in Sec. IV. The concluding remarks are provided in the last section of the paper. Appendix A provides the descriptions of these problems. Appendix B gives the evaluation of the dependency of the scale parameter k on the nature of the LSF and the probability distribution of the LSF. Appendix C provides an evaluation of the dependency of the performance of the proposed method on the probability distribution types of the input random variables.

II. Existing Methods

A. Classical Tail Modeling

Consider the LSF $y(\boldsymbol{x})$, where $\boldsymbol{x}$ is the vector of random variables. For a given threshold value of F_t (see Fig. 1), the region above the threshold (i.e., the tail portion) can be approximated by using a proper tail model. Tail models are used to predict the probabilities at unobserved levels by using the probabilities at observed levels through extrapolation.

The tail models used in the literature include generalized Pareto distribution [14], generalized extreme value distribution [15], and polynomial approximation of the reliability index itself or the logarithm of the reliability index [8]. For instance, generalized Pareto distribution approximates the conditional excess distribution of $F_z(z)$, where $z = y - y_t$, by using the following equation:

$$F_z(z) = \begin{cases} 1 - \left\langle 1 + \frac{\xi}{\sigma} z \right\rangle_+^{-(1/\xi)} & \text{if } \xi \neq 0 \\ 1 - \exp\left(-\frac{z}{\sigma}\right) & \text{if } \xi = 0 \end{cases} \tag{1}$$

where $\langle A \rangle_+ = \max(0, A)$, $z \geq 0$, and $F_z(z)$ is the generalized Pareto distribution with shape and scale parameters ξ and σ, respectively. These tail model parameters are usually found through the maximum likelihood method or the least square method [8]. Then, the CDF value above the threshold (i.e., $z \geq 0$) is expressed in terms of the conditional excess distribution, $F_z(z)$, via

$$F(y) = F_t + (1 - F_t) F_z(y - y_t) \tag{2}$$

Once the CDF $F(y)$ is obtained, the probability of failure P_f and the generalized reliability index [16] β can be estimated from

$$P_f = 1 - F(y = 0); \qquad \beta = \Phi^{-1}(1 - P_f) \tag{3}$$

where Φ is the CDF of a standard normal random variable.

Similarly, if a polynomial approximation of the reliability index is used, then the reliability index is related to the exceedance value z through a suitable polynomial and the coefficients of this polynomial are usually found through the least square method [8].

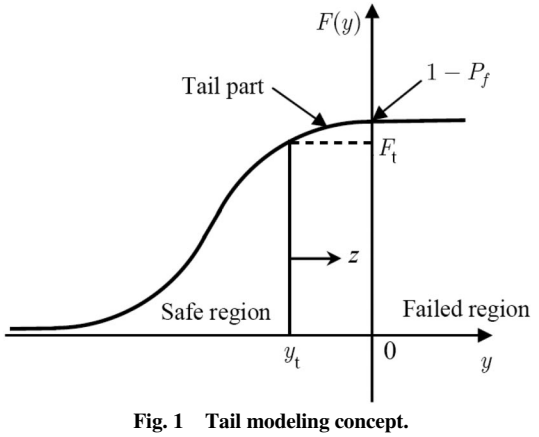

Fig. 1 Tail modeling concept.

The CTM method is based on the following three-step procedure:

1) N samples of the LSF $y(\boldsymbol{x})$ are generated through MCS (or Latin hypercube sampling). In structural mechanics problems, the samples of the input random variables, $\boldsymbol{x}$, are first generated from the given distribution types, and then the samples of the random LSF are calculated through structural analyses. Because structural analyses are usually performed through computationally expensive simulations (e.g., finite element analysis), the value of N is selected based on allowable computational budget. In this paper, the number of samples is limited to $N = 500$.

2) A threshold value, F_t, is selected and the tail samples are identified. For instance, if the threshold value is chosen as $F_t = 0.90$, the number samples in the tail region is $N_t = (1 - F_t)N = 50$. The threshold value F_t is found to have a substantial effect on the reliability predictions, and empirical values have been proposed [5–7]. Boos [5] suggested using $N_t/N = 0.2$ for $50 \leq N \leq 500$ and $N_t/N = 0.1$ for $500 < N \leq 5000$. Hasofer [6] showed that using $N_t \approx 1.5\sqrt{N}$ works well for most distributions. Caers and Maes [7] proposed that the optimal N_t value can be selected to minimize the mean square error, which can be estimated using bootstrap technique. For $N = 500$ (as used in this paper), Boos's empirical formula yields $N_t = 100$, whereas Hasofer's formula yields $N_t = 34$. In this paper, $N_t = 50$ is used as a compromise between the two.

3) The parameters in the tail model are estimated. If generalized Pareto distribution, generalized extreme value distribution, or another proper distribution is used as a tail model, then the tail model parameters can be found either by using the maximum likelihood method or the least square method [8]. If polynomial approximation of the reliability index (or logarithm of the reliability index) is used, the tail model parameters are usually found through the least square method [8]. In this paper, polynomial approximations (both linear and quadratic) of the reliability index and logarithm of the reliability index are used.

Even though the CTM method is an efficient reliability prediction method, the efficiency of tail modeling can further be increased. This paper proposes that the MCMC method with MH algorithm can be blended with CTM. The MCMC method with MH algorithm is described in the next section.

B. Markov Chain Monte Carlo

MCMC method with MH algorithm can be used to generate a sequence of sampling points from a target probability distribution for which direct sampling is not trivial [17,18]. MCMC is widely used in conjunction with importance sampling methods for reliability calculation. The main role of MCMC is to construct asymptotically optimal importance sampling density [19] and keep the subsequent sampling within the region of interest (failure region for importance sampling, tail region for tail modeling, etc.). The first step in MCMC is finding a starting point (or a starting state) in the region of interest. The starting point can be determined based on engineering judgment, random sampling, or other means. Then, the subsequent sampling within the region of interest can be performed based on the following procedure, which is repeated until the allowable number of samples is reached:

1) Assume that the current point (or current state) is $\boldsymbol{x}^i_{\text{cur}}$. Generate a candidate point (or candidate state) $\boldsymbol{x}_{\text{can}}$ around the current point by performing a random walk using a proposal distribution $q(\boldsymbol{x}_{\text{can}}|\boldsymbol{x}^i_{\text{cur}})$. The proposal distribution is chosen to be symmetric. Gaussian distribution is the most commonly used proposal distribution [19].

2) Determine whether the candidate point lies in the region of interest. If not, nullify the joint PDF of the candidate point.

3) Compute the ratio of the joint PDF values at the candidate and the current points, $r = f(\boldsymbol{x}_{\text{can}})/f(\boldsymbol{x}_{\text{cur}})$. If $r \geq 1$, then the candidate point is accepted as the next point (or next state). If $r < 1$, then the candidate point is accepted as the next state with probability r, and the current state is accepted as the next state with probability $(1 - r)$.

The effectiveness of MCMC is affected by the choice of proposal distribution parameters that control the step size of random walks. The use of a large step size allows large coverage of the sampling space and may lead to identification of multiple disconnected or weakly connected regions of interest, whereas the probability of

getting repeated states is increased. On the other hand, the use of a small step size reduces the probability of getting repeated states but it may increase the correlation between successive states and retards the robustness of the algorithm.

Proposal parameters are often chosen manually, through trial and error, whereas this would be impractical for many problems considering the numerical cost associated with that practice. There has been significant progress for optimum choice of the proposal distribution parameters in recent years and it is still an active research area. Rosenthal [20] showed that if the target distribution is $N(0, \sum)$ for an n_{var}-dimensional covariance matrix $\sum$, and the proposal distribution is $N(0, \sum_p)$, then the optimal covariance matrix can be found as

$$\sum_p = \frac{2.38^2}{n_{\text{var}}} \sum \tag{4}$$

The above formula is suitable when the target distribution is normal [20], whereas probability distribution of the tail part is not necessarily normal. Therefore, in this paper the proposal distribution formula is modified as explained in the next section.

III. Proposed Method

The LSF evaluation budget is taken as 500 based on our earlier work [9,10] and others [8,11]. In this paper, this computational budget is divided into two sets. The first set of LSF evaluations is used for estimating the threshold value of the LSF as well as finding starting point(s) for MCMC sampling. The second set is used to perform subsequent sampling from tail part of the CDF through MCMC. After the tail samples are generated, polynomial approximations (both linear and quadratic) of the reliability index and logarithm of the reliability index are constructed, and reliability prediction is performed through extrapolation.

In the first set, the number of LSF evaluations is limited to 100. Therefore, 100 samples are generated in random variable space based on the probability distributions of the random variables through MCS, and LSF evaluations are performed. The LSF values are sorted in ascending order. F_t quantile defines the threshold value of LSF, y_t. The last 10 samples are tail samples and these 10 samples are used as starting points for MCMC sampling. It must be noted that the tail region found using a small number of samples may not represent the true tail region; therefore, some of these 10 samples may not belong to the true tail region. The use of multiple starting points allows sampling from multiple disconnected tail regions as shown in Fig. 2 for the tuned mass damper example problem (one of the numerical example problems used in this paper).

In the second set, the number of LSF evaluations is limited to 400. Corresponding to each starting point, 40 subsequent samples are generated from the tail part of the CDF through MCMC with MH algorithm. MCMC samples are generated from the tail region only by nullifying the joint PDF in the nontail region and by generating samples in the tail region according to the original joint PDF. In MCMC, normal distribution with zero mean is used as the proposal distribution. The proposal distribution formula suggested by Rosenthal [20] is suitable when the target distribution is normal. For a general case, probability distribution of the tail part is not necessarily normal. Therefore, in this paper the proposal distribution formula suggested by Rosenthal [20] is modified as follows to compute the covariance matrix of the proposal distribution:

$$\sum_p = k^2 \frac{2.38^2}{n_{\text{var}}} \sum \tag{5}$$

where $\sum$ is the covariance matrix of the random variables. In this study, the value of k is varied and the optimal value of k is obtained for various example problems with a varying number of variables, and an approximate relationship is obtained for the optimal value of k in terms of the number of random variables. Note that Eq. (5) represents an ad-hoc correction for non-Gaussian application, without a mathematical derivation.

According to the above procedure, overall 410 tail samples are generated. After these tail samples are generated, polynomial approximations (both linear and quadratic) of the reliability index and logarithm of the reliability index are constructed, and reliability prediction is performed through extrapolation. That is, the following eight polynomial approximation types are constructed, and then the reliability predictions are performed.

1) Linear approximation between the exceedance and the reliability index: $\beta_1(z) = c_0 + c_1 z$. Once the approximation is constructed, the reliability index is predicted through extrapolation. The reliability index prediction is obtained from $\beta^L_{\text{lin-lin}} = \beta_1(z = -y_t)$.

2) Quadratic approximation between the exceedance and the reliability index: $\beta_2(z) = c_0 + c_1 z + c_2 z^2$. The reliability index prediction is obtained from $\beta^Q_{\text{lin-lin}} = \beta_2(z = -y_t)$.

3) Linear approximation between the exceedance and the logarithm of reliability index: $\ln \beta_3(z) = c_0 + c_1 z$. The reliability index prediction is obtained from $\beta^L_{\text{log-lin}} = \exp[\ln \beta_3(z = -y_t)]$.

4) Quadratic approximation between the exceedance and the logarithm of reliability index: $\ln \beta_4(z) = c_0 + c_1 z + c_2 z^2$. The reliability index prediction is obtained from $\beta^Q_{\text{log-lin}} = \exp[\ln \beta_4(z = -y_t)]$.

5) Linear approximation between the logarithm of the exceedance and the reliability index: $\beta_5(z) = c_0 + c_1 \ln z$. The reliability index prediction is obtained from $\beta^L_{\text{lin-log}} = \beta_5(z = -y_t)$.

6) Quadratic approximation between logarithm of the exceedance and the reliability index: $\beta_6(z) = c_0 + c_1 \ln z + c_2 (\ln z)^2$. The reliability index prediction is obtained from $\beta^Q_{\text{lin-log}} = \beta_6(z = -y_t)$.

7) Linear approximation between the logarithm of the exceedance and the logarithm of reliability index: $\ln \beta_7(z) = c_0 + c_1 \ln z$). The reliability index prediction is obtained from $\beta^L_{\text{log-log}} = \exp[\ln \beta_7(z = -y_t)]$.

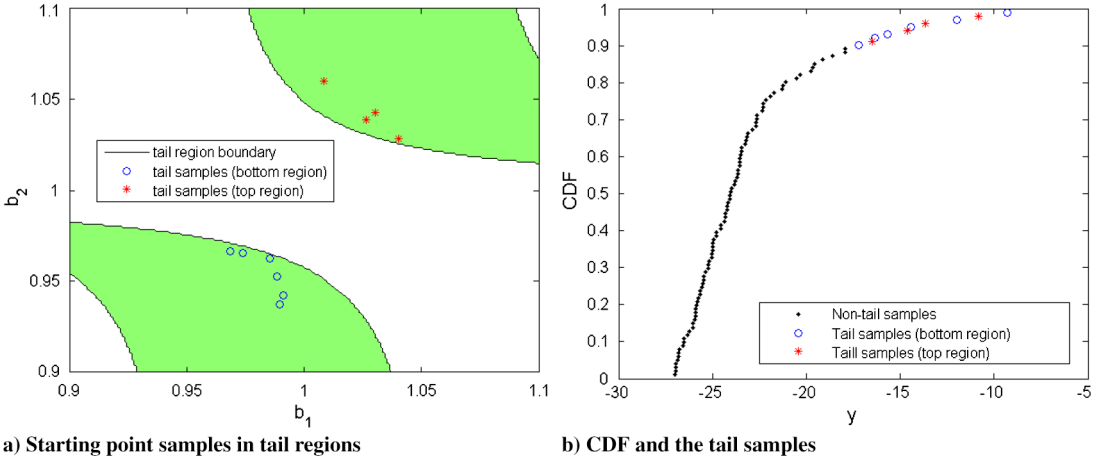

a) Starting point samples in tail regions b) CDF and the tail samples

Fig. 2 Sampling from multiple disconnected tail regions by using multiple starting points.

Table 1 The numerical example problems used in this study

ID	Problem	Number of variables
1	Simple example	2
2	Branin–Hoo	2
3	Camelback	2
4	Tuned mass damper	2
5	Central crack	4
6	Rotating disk	6
7	Rosenbrock (6 var.)	6
8	Dixon–Price (6 var.)	6
9	Rosenbrock (9 var.)	9
10	Dixon–Price (12 var.)	12

Table 2 Statistical properties of the random variables in the illustrative example

Random variable	Distribution	Mean	Standard deviation
R	Normal	μ_R	6
C	Normal	100	8

8) Quadratic approximation between the logarithm of the exceedance and the logarithm of reliability index: $\ln \beta_8(z) = c_0 + c_1 \ln z + c_2 (\ln z)^2$). The reliability index prediction is obtained from $\beta^{Q}_{\log-\log} = \exp[\ln \beta_8(z = -y_t)]$.

IV. Application to Example Problems

The accuracy of the proposed method is evaluated by using numerical example problems as well as reliability prediction of a horizontal axis wind turbine. Because the proposed method is a sampling-based method, the reliability index predictions may differ from a particular set of sampling points to another. To reduce the effect of random sampling, the whole process is repeated for 10,000 times by using different sets of sampling points and the root mean square error (RMSE) is evaluated. Reliability index predictions obtained through classical MCS with 10^9 samples are used as basis in comparison.

A. Application to Numerical Example Problems

Numerical example problems with a different number of variables are used in this study as listed in Table 1. Descriptions of these problems are provided in Appendix A. For all problems, three different levels of reliability indices are used by adjusting the problem parameters as explained in Appendix A.

Example problem 1 is a two-variable simple problem with a linear LSF and is used to illustrate the proposed method. The LSF of this example problem is given as

$$Y = R - C \tag{6}$$

where R denotes the response (e.g., stress), C denotes the capacity (e.g., strength), and both are random variables. Note that the positive values of this LSF denote failure. The statistical properties of these random variables are provided in Table 2. The mean value of the response μ_R can be changed to obtain various levels of reliability index values. For this problem, the actual reliability index can be obtained easily from Eq. (7) as the LSF is linear and both random variables follow normal distribution. In Eq. (7), μ and σ correspond to the mean and standard deviation of the corresponding quantity, respectively.

$$\beta = \frac{\mu_C - \mu_R}{\sqrt{\sigma_C^2 + \sigma_R^2}} = \frac{100 - \mu_R}{\sqrt{8^2 + 6^2}} = 10 - \frac{\mu_R}{10} \tag{7}$$

First, the CTM is used to predict the reliability index by using eight different polynomial approximation types (namely, $\beta^{L}_{\text{lin}-\text{lin}}$, $\beta^{Q}_{\text{lin}-\text{lin}}$, $\beta^{L}_{\text{lin}-\text{log}}$, $\beta^{Q}_{\text{lin}-\text{log}}$, $\beta^{L}_{\text{log}-\text{lin}}$, $\beta^{Q}_{\text{log}-\text{lin}}$, $\beta^{L}_{\text{log}-\text{log}}$, and $\beta^{Q}_{\text{log}-\text{log}}$). The RMSEs are calculated and reported in Table 3. The RMSE values shown in bold fonts correspond to the smallest value in each row. It is found that $\beta^{L}_{\text{lin}-\text{lin}}$ approximation type provides the most accurate reliability predictions. This is not surprising as the LSF is linear and the random variables follow normal distribution.

Next, the proposed method (MCMC-based tail modeling [MCMC-TM]) is used to predict the reliability index by using eight different polynomial approximation types. In MCMC-TM, the proposal distribution scale parameter k plays an important role in the reliability index predictions. Eight different k values are used in the reliability

Table 3 Root mean square errors of CTM predictions

μ_R	β_{act}	$\beta^{L}_{\text{lin}-\text{lin}}$	$\beta^{Q}_{\text{lin}-\text{lin}}$	$\beta^{L}_{\text{lin}-\text{log}}$	$\beta^{Q}_{\text{lin}-\text{log}}$	$\beta^{L}_{\text{log}-\text{lin}}$	$\beta^{Q}_{\text{log}-\text{lin}}$	$\beta^{L}_{\text{log}-\text{log}}$	$\beta^{Q}_{\text{log}-\text{log}}$
70	3.0	**0.237**	0.337	0.813	0.446	0.465	0.398	0.805	0.376
60	4.0	**0.388**	1.038	1.702	1.113	1.825	3.263	1.664	0.889
50	5.0	**0.548**	2.175	2.622	1.872	4.968	34.603	2.554	1.467

Boldface numbers show the minimum error values in each row.

Table 4 Root mean square errors of MCMC-TM predictions ($\beta^{L}_{\text{lin}-\text{lin}}$ is used as the approximation type)

μ_R	β_{act}	$k = 0.1$	$k = 0.25$	$k = 0.5$	$k = 0.75$	$k = 1$	$k = 1.25$	$k = 1.5$	$k = 2$
70	3.0	0.441	0.279	**0.231**	0.234	0.263	0.298	0.327	0.392
60	4.0	0.700	0.429	**0.344**	0.363	0.399	0.467	0.515	0.634
50	5.0	0.966	0.589	**0.473**	0.494	0.553	0.631	0.739	0.875

Boldface numbers show the minimum error values in each row.

Table 5 The impact of the proposal distribution scale parameter on sampling point scatter in tail region[a]

Proposal dist. scale parameter, k	0.1	0.25	0.5	0.75	1	1.25	1.5	2
Number of nonrepeated samples	321	229	141	94	68	51	41	29

The number of samples used to construct the tail model is 410.

[a]To reduce the effect of random sampling, the whole procedure is repeated 10,000 times with different samples, and the average values are reported in the table.

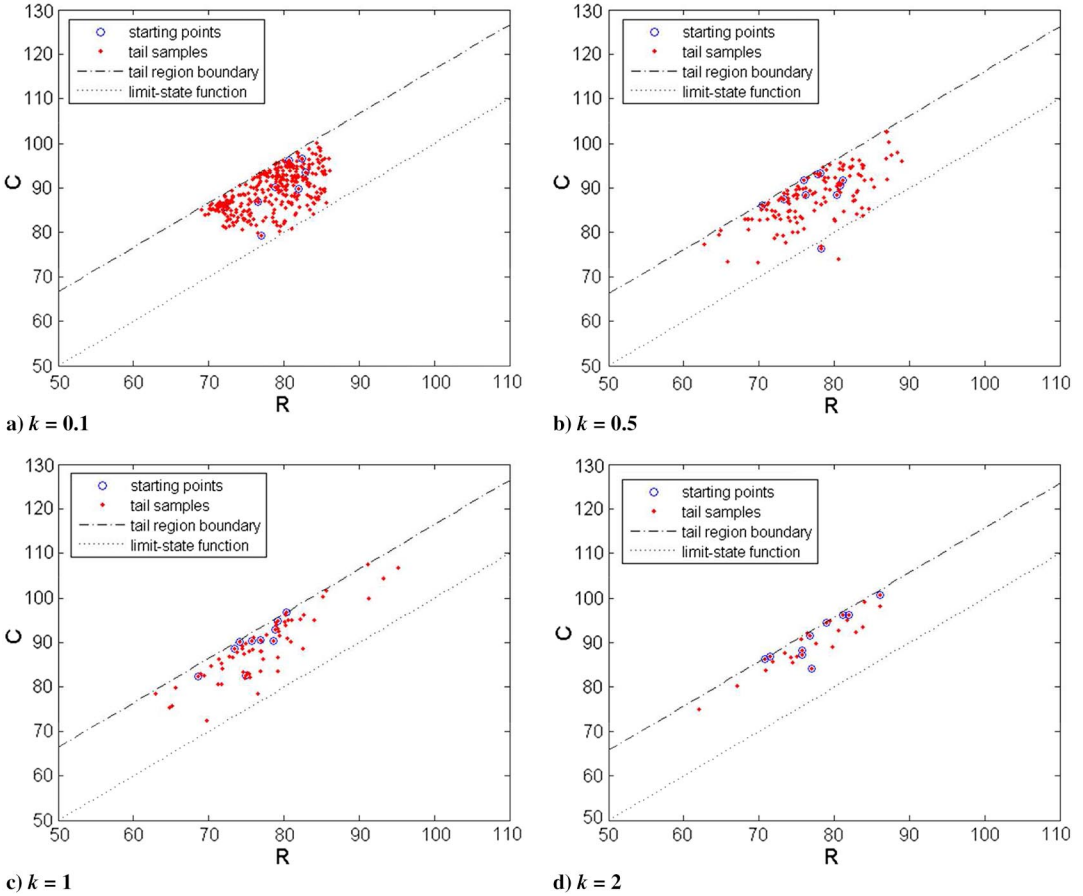

Fig. 3 The effect of the proposal distribution scale parameter on sampling point scatter in tail region.

Table 6 Root mean square errors of MCMC-TM predictions in a reduced range of proposal distribution scale parameter values

μ_R	β_{act}	$k = 0.25$	$k = 0.3$	$k = 0.35$	$k = 0.4$	$k = 0.45$	$k = 0.5$	$k = 0.55$	$k = 0.6$	$k = 0.65$	$k = 0.7$	$k = 0.75$
70	3.0	0.279	0.255	0.242	0.233	0.231	0.231	**0.225**	0.226	0.230	0.235	0.234
60	4.0	0.429	0.393	0.373	0.360	0.348	**0.344**	0.345	0.349	0.350	0.354	0.363
50	5.0	0.589	0.534	0.507	0.486	0.476	**0.473**	0.475	0.476	0.484	0.491	0.494

Boldface numbers show the minimum error values in each row.

index predictions (see Table 4). For the eight different k values considered, it is found that $\beta^{L}_{\text{lin-lin}}$ approximation type provides the most accurate reliability predictions as in the case of CTM. It must be noted that the polynomial approximation type that provides the most accurate reliability predictions in CTM does not necessarily provide the most accurate reliability predictions in MCMC-TM. Table 4 shows that the most accurate predictions are achieved when the proposal distribution scale parameter is taken as $k = 0.5$.

The scatter of the sampling points in tail region has a direct influence on the reliability prediction through tail modeling. Therefore, the effect of the proposal distribution scale parameter on the scatter of sampling points in the tail region is also investigated. For this investigation, $\mu_R = 70$ is used. Table 5 and Fig. 3 show that as the proposal distribution scale parameter increases, it is possible to sample from a wide range of the random variable space, and this is an advantage. It is also found, on the other hand, that as the proposal distribution scale parameter increases, the number of repetitive samples increases, and this is a drawback. Therefore, the value of the scale parameter needs to be properly chosen for an accurate reliability estimation.

Then, the optimal value of the proposal distribution scale parameter is determined. Based on the results shown in Table 4, the optimal value of k is predicted to be in the [0.25, 0.75] range (for all reliability levels and for this particular problem of interest). The value of k is varied between 0.25 and 0.75 in 0.05 increments, and reliability index predictions are performed. The RMSE values are provided in Table 6. Because a finite number of sampling sets is used in RMSE calculations, the RMSE values are subject to numerical noise. To eliminate this numerical noise, response surface modeling is used to determine the optimal value of k.

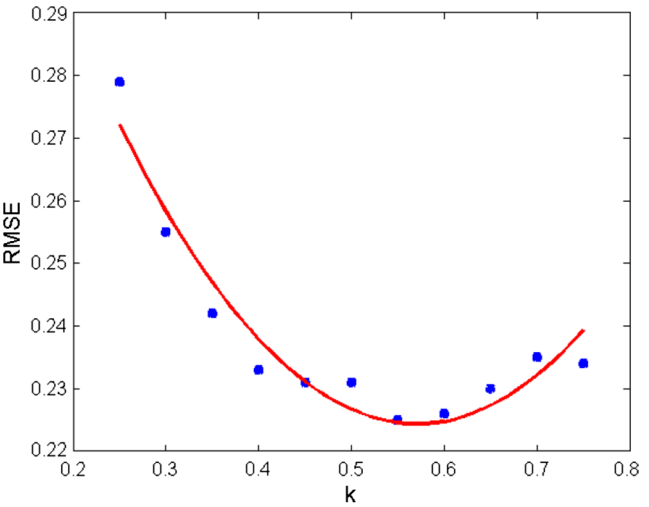

Fig. 4 Change of RMSE over different k values (for $\mu_R = 70$) and the response surface model fitted.

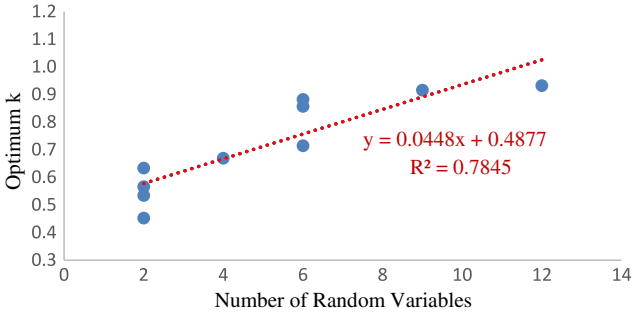

Fig. 5 Variation of the optimum k value with respect to the number of random variables.

A quadratic response surface is fitted to RMSE values in terms of the proposal distribution scale parameter (see Fig. 4), and the constructed response surface is used to determine the optimal value of k. For this simple example problem with $\mu_R = 70$, the optimal value of the proposal distribution scale parameter is found to be $k^* = 0.5707$. Similarly, the optimal value of k is found as $k^* = 0.5662$ for $\mu_R = 60$, and $k^* = 0.5613$ for $\mu_R = 50$.

The overall procedure outlined above for the Example Problem 1 is repeated for all reliability levels of all example problems, and the optimum k values obtained are given in Table 6. It is found that as the number of random variables in the problem increases, the optimum k value also increases. It is also observed that there is no clear correlation between the reliability level of the problem and the optimum k value. Therefore, the average values of the optimum k values are computed over three different reliability levels for all example problems, and these average values are used to generate an approximate relationship between the optimum k value and the number of random variables.

The dependency of the scale parameter k on the nature of the LSF and the statistical properties of the LSF is analyzed. The details of this analysis are provided in Appendix B. The linearity and the roughness of the LSF are used as measures of the nature of the LSF. The coefficient of variation (c.o.v.), skewness, and kurtosis are used as key statistical properties of the limit state function. It is found that there is no linear relationship between these measures and the scale parameter k.

The variation of the optimum k value (the average value evaluated over three different reliability levels) with respect to the number of variables over all example problems is shown in Fig. 5. A linear response surface is constructed between the number of random variables (n_{var}) and optimum k value (k^*). It is found that an approximate relationship $k^* = 0.4877 + 0.0448 n_{\text{var}}$ can be constructed. This approximate relationship will be used in the next section, where the proposed method is applied to the reliability prediction of a horizontal axis wind turbine.

The comparison of the accuracy of CTM and MCMC-TM predictions over all example problems is provided in Table 8, where the smaller RMSE value in each row is shown in bold fonts for ease of

Table 7 Optimum k values for all example problems

Problem ID	n_{var}	For β_{low}	For β_{med}	For β_{high}	Average
1	2	0.5707	0.5662	0.5613	0.5661
2	2	0.5051	0.7499	0.6458	0.6336
3	2	0.5368	0.5639	0.5036	0.5348
4	2	0.3722	0.4933	0.4925	0.4527
5	4	0.6669	0.6690	0.6737	0.6699
6	6	0.7255	0.7168	0.7030	0.7151
7	6	0.7922	0.5869	1.2685	0.8825
8	6	0.6373	0.9032	1.0320	0.8575
9	9	0.8521	0.5801	1.3150	0.9157
10	12	0.7988	0.9611	1.0366	0.9322

Table 8 Comparison of the RMSE of CTM and MCMC-TM for all example problems

Problem ID	n_{var}	Rel. index, β	RMSE for CTM	Approach for CTM	RMSE for MCMC-TM	Approach for MCMC-TM
1	2	3.00	0.237	$\beta^L_{\text{lin}-\text{lin}}$	**0.225**	$\beta^L_{\text{lin}-\text{lin}}$
		4.00	0.388	$\beta^L_{\text{lin}-\text{lin}}$	**0.344**	$\beta^L_{\text{lin}-\text{lin}}$
		5.00	0.548	$\beta^L_{\text{lin}-\text{lin}}$	**0.473**	$\beta^L_{\text{lin}-\text{lin}}$
2	2	3.03	0.333	$\beta^Q_{\text{log}-\text{log}}$	**0.265**	$\beta^Q_{\text{log}-\text{log}}$
		4.00	0.509	$\beta^Q_{\text{log}-\text{log}}$	**0.480**	$\beta^Q_{\text{lin}-\text{log}}$
		5.00	0.908	$\beta^Q_{\text{lin}-\text{log}}$	**0.630**	$\beta^Q_{\text{lin}-\text{log}}$
3	2	2.95	0.266	$\beta^Q_{\text{lin}-\text{log}}$	**0.211**	$\beta^Q_{\text{lin}-\text{log}}$
		4.00	0.566	$\beta^Q_{\text{lin}-\text{log}}$	**0.395**	$\beta^Q_{\text{lin}-\text{log}}$
		5.05	0.764	$\beta^Q_{\text{lin}-\text{log}}$	**0.532**	$\beta^Q_{\text{lin}-\text{log}}$
4	2	3.03	0.329	$\beta^Q_{\text{log}-\text{log}}$	**0.191**	$\beta^Q_{\text{lin}-\text{lin}}$
		3.42	0.434	$\beta^L_{\text{lin}-\text{lin}}$	**0.376**	$\beta^L_{\text{lin}-\text{lin}}$
		4.46	1.179	$\beta^L_{\text{log}-\text{lin}}$	**1.010**	$\beta^L_{\text{log}-\text{lin}}$
5	4	3.01	0.241	$\beta^L_{\text{lin}-\text{lin}}$	**0.241**	$\beta^L_{\text{lin}-\text{lin}}$
		4.01	0.396	$\beta^L_{\text{lin}-\text{lin}}$	**0.369**	$\beta^L_{\text{lin}-\text{lin}}$
		5.01	0.546	$\beta^L_{\text{lin}-\text{lin}}$	**0.512**	$\beta^L_{\text{lin}-\text{lin}}$
6	6	3.06	**0.241**	$\beta^L_{\text{lin}-\text{lin}}$	0.247	$\beta^L_{\text{lin}-\text{lin}}$
		4.05	0.431	$\beta^L_{\text{lin}-\text{lin}}$	**0.374**	$\beta^L_{\text{lin}-\text{lin}}$
		5.08	0.650	$\beta^L_{\text{lin}-\text{lin}}$	**0.540**	$\beta^L_{\text{lin}-\text{lin}}$
7	6	3.03	0.284	$\beta^Q_{\text{log}-\text{log}}$	**0.259**	$\beta^Q_{\text{lin}-\text{log}}$
		4.03	**0.510**	$\beta^Q_{\text{log}-\text{log}}$	0.547	$\beta^Q_{\text{log}-\text{log}}$
		5.03	**0.827**	$\beta^Q_{\text{log}-\text{log}}$	0.948	$\beta^Q_{\text{lin}-\text{log}}$
8	6	3.00	0.267	$\beta^Q_{\text{log}-\text{log}}$	**0.238**	$\beta^Q_{\text{lin}-\text{log}}$
		4.02	0.533	$\beta^Q_{\text{log}-\text{log}}$	**0.495**	$\beta^Q_{\text{lin}-\text{log}}$
		5.04	1.100	$\beta^Q_{\text{log}-\text{log}}$	**0.808**	$\beta^Q_{\text{lin}-\text{log}}$
9	9	3.02	0.289	$\beta^Q_{\text{log}-\text{log}}$	**0.271**	$\beta^Q_{\text{lin}-\text{log}}$
		4.04	**0.526**	$\beta^Q_{\text{log}-\text{log}}$	0.553	$\beta^Q_{\text{log}-\text{log}}$
		5.09	**0.829**	$\beta^Q_{\text{log}-\text{log}}$	0.950	$\beta^Q_{\text{lin}-\text{log}}$
10	12	3.05	0.284	$\beta^Q_{\text{log}-\text{log}}$	**0.267**	$\beta^Q_{\text{lin}-\text{log}}$
		4.02	**0.521**	$\beta^Q_{\text{log}-\text{log}}$	0.523	$\beta^Q_{\text{lin}-\text{log}}$
		5.07	1.072	$\beta^Q_{\text{log}-\text{log}}$	**0.834**	$\beta^Q_{\text{lin}-\text{log}}$

Boldface numbers show the minimum error values in each row.

Table 9 General characteristics of Risoe wind turbine

Number of blades	3
Turbine diameter	19 m
Rotational speed	47.5 rpm
Cut-in wind speed	4 m/s
Control type	*Stall*
Rated power	100 kW
Root extension	2.3 m
Blade set angle	1.8 deg
Maximum twist	15 deg
Root chord	1.09 m
Tip chord	0.45 m
Airfoil	NACA 63-4xx series

comparison. It is found that MCMC-TM predictions are more accurate than CTM predictions at all reliability levels when the number of variables is less than or equal to four. For the six-variable problems, MCMC-TM predictions are more accurate than CTM predictions for six cases out of nine. For the nine-variable problem, MCMC-TM prediction is more accurate than CTM prediction at only one reliability level. Finally, for the 12-variable problem, MCMC-TM predictions are more accurate than CTM predictions at two reliability levels.

Evaluation of the dependency of the performance of the proposed method on the probability distribution types of the input random variables is explored in Appendix C. It is found that the performance of MCMC-TM is not dependent on the probability distribution types of the input random variables, and this is in fact a good property possessed by the tail modeling methods.

B. Application to Wind Turbine Reliability Prediction

The proposed method is also applied to reliability prediction of the Risoe wind turbine, which is a 100 kW horizontal-axis wind turbine developed by Denmark Technical University National Laboratory for Sustainable Energy to be used for field testing purposes. Table 9 provides the geometrical characteristics of Risoe wind turbine (taken from Ceyhan et al. [21]). Risoe wind turbine blades are twisted and tapered (see Fig. 6), and use NACA 63-4xx series airfoils.

Table 10 Random variables for Risoe wind turbine problem

ID	Random variable	Distribution	Mean	Standard deviation
RV1	Turbine radius	Normal	9.5 m	0.01 m
RV2	Rotational speed	Normal	47.5 rpm	0.03 rpm
RV3	Blade set angle	Normal	1.8 deg	0.05 deg
RV4	Root chord	Normal	1.09 m	0.01 m

The reliability of the wind turbine is evaluated by its capability of producing 100 kW power output at 13.5 m/s wind speed. The power generated by the wind turbine is evaluated using WT_Perf software (a free software developed by the U.S. National Renewable Energy Laboratory), which uses blade element momentum theory (BEMT).

BEMT is one of the oldest and most commonly used methods for evaluating the aerodynamic performance of wind turbines. BEMT is a combination of the blade element theory and momentum theory [22]. Even though the theory is based on many assumptions, it still provides satisfactory results at low wind speed values [23]. In this theory, the flow is assumed to be continuous, homogeneous, steady state, incompressible, and axisymmetric and the turbulence effects are ignored. In this study, the number of blade elements is taken as 10.

The LSF of this example problem is given as

$$Y = P_{\text{out}}(\boldsymbol{x}) - P_{\text{crit}} \tag{8}$$

where P_{out} is the power output of the wind turbine, $\boldsymbol{x}$ is the random variable vector, and P_{crit} is the critical value of the power output (taken as 100 kW). For this problem, the random variables are the turbine radius, the rotational speed, the blade set angle, and the root chord. Table 10 gives the statistical properties of the random variables.

Two different cases of this problem are considered to obtain two different reliability levels. For the first case RV1 through RV4 are all taken as random variables, whereas for the second case RV1 through RV3 are taken as random variables. The reliability indices corresponding to the first and the second cases are computed as $\beta = 3.69$ and $\beta = 4.92$, respectively, through MCS with a sample size of 10^7.

The procedure followed for the numerical example problems is repeated for the wind turbine problem. First, RMSE values of

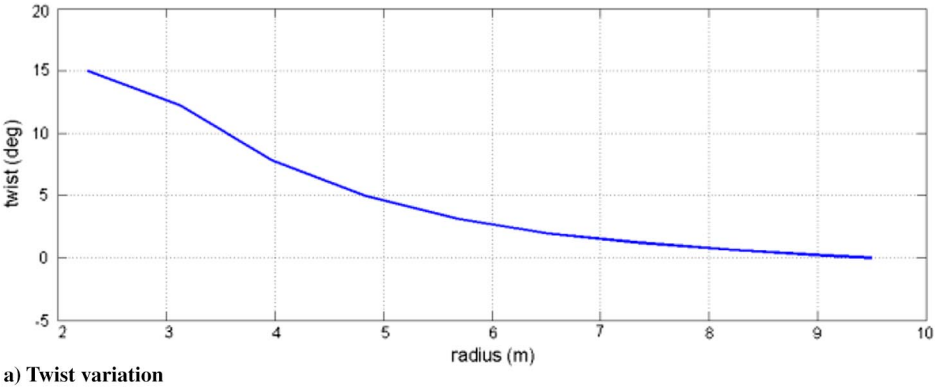

a) Twist variation

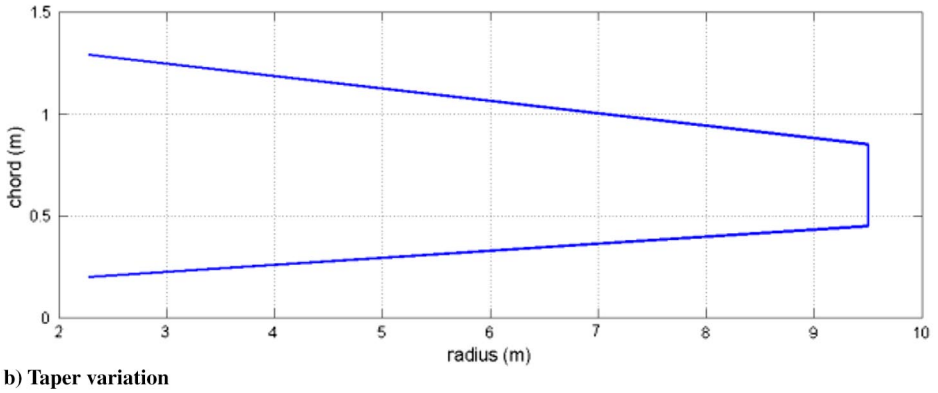

b) Taper variation

Fig. 6 Twist and taper variation of Risoe wind turbine blades over the chord.

Table 11 Root mean square errors of MCMC-TM predictions in a reduced range of proposal distribution scale parameter values (wind turbine problem)

n_{var}	β_{act}	$k = 0.5$	$k = 0.55$	$k = 0.6$	$k = 0.65$	$k = 0.7$	$k = 0.75$	$k = 0.8$	$k = 0.85$	$k = 0.9$	$k = 0.95$	$k = 1.00$
4	3.69	0.338	0.336	0.326	0.330	**0.316**	0.320	0.338	0.328	0.349	0.362	0.351
n_{var}	β_{act}	$k = 0.25$	$k = 0.3$	$k = 0.35$	$k = 0.4$	$k = 0.45$	$k = 0.5$	$k = 0.55$	$k = 0.6$	$k = 0.65$	$k = 0.7$	$k = 0.75$
3	4.92	0.632	0.561	0.543	0.522	0.491	0.480	0.475	**0.472**	0.491	0.474	0.489

Boldface numbers show the minimum error values in each row.

MCMC-TM predictions are computed for eight different k values (i.e., $k = 0.1$, $k = 0.25$, $k = 0.5$, $k = 0.75$, $k = 1$, $k = 1.25$, $k = 1.5$, and $k = 2$). The smallest RMSE value is obtained for $k = 0.5$ for the three-variable case, whereas the smallest RMSE value is obtained for $k = 0.75$ for the four-variable case. Based on these results, the optimal value of k is predicted to be in the [0.25, 0.75] range for the three-variable case, and in the [0.5, 1.0] range for the four-variable case. Next, the value of k is varied between its lower and upper bounds in 0.05 increments, and reliability index predictions are performed. The RMSE values of MCMC-TM predictions in the reduced k range are given in Table 11.

Then, quadratic response surfaces are fitted to RMSE values in terms of the proposal distribution scale parameter for both cases, and the constructed response surfaces are used to determine the optimal value of k. Table 12 shows the optimum k values for two reliability levels as well as the prediction of the optimal k value by using the approximate relationship obtained earlier ($k^* = 0.4877 + 0.0448 n_{var}$). It is seen that the approximate value and the optimum value obtained are in good agreement. Finally, the accuracies of CTM and MCMC-TM predictions for this problem are compared. Table 13 shows that MCMC-TM predictions are more accurate than CTM predictions for both of the reliability levels of this problem.

C. Confidence Intervals of the Reliability Estimations by Using Bootstrap Method

The errors of the reliability index predictions are computed by using the actual values of the reliability indices, which are unknown for the practical problems. The confidence intervals of the reliability estimations provide an estimation of the expected error. As noted by Picheny et al. [24], derivation of an analytical formula for the confidence intervals is a very challenging task. To overcome this problem, bootstrap method is used to assess the confidence intervals in this study.

Bootstrap method is an efficient numerical method to estimate the distribution of a statistical parameter from a sample set of results [25]. The main idea of bootstrapping method is to generate a number of bootstrap samples by re-sampling with replacement from the original samples, and then approximating the distribution of the statistical parameter of interest (e.g., mean, standard deviation, probability of failure, etc.) from the bootstrap samples. As the re-sampling procedure is based on selecting data randomly with replacement, the statistical properties of the bootstrap samples are different from that of the original samples. Therefore, for any bootstrap samples, the value of the statistical parameter of interest would take different values, allowing estimation of the statistical distribution of the statistical parameter of interest. It was suggested that the size of the samples (N) should be larger than 100 to obtain reliable results [26]. In this study, we use $N = 500$ samples. It was recommended that the number of bootstrap sample sets (p) should be large enough (typically between 500 and 5000) so that the major source of uncertainty would come from the original sample [24]. In this study, we use $p = 1000$ set of bootstrap samples. The framework for the bootstrap method is shown in Fig. 7. The reader may refer to [24–26] for details of bootstrap method.

The 95% confidence intervals for the MCMC-TM predictions and the RMSE value calculated based on the actual reliability index value are given in Table 14. Because the 95% confidence intervals correspond to plus/minus two standard deviations away from the mean (for a normal distribution), we compare the confidence interval divided by four to the RMSE values. Note that for a non-Gaussian response, plus/minus two standard deviations may not correspond to 95% confidence. It is observed that the confidence intervals computed through the bootstrap method have good agreement with the RMSE values, which are unavailable for practical problems.

Table 12 Optimum k values and comparison to the approximate value

n_{var}	β_{act}	k^*	$k^* = 0.4877 + 0.0448 n_{var}$
4	3.69	0.689	0.667
3	4.92	0.603	0.622

Table 13 Comparison of the RMSE of CTM and MCMC-TM for the wind turbine problem

n_{var}	Rel. index, β	RMSE for CTM	Approach for CTM	RMSE for MCMC-TM	Approach for MCMC-TM
4	3.69	0.376	$\beta^L_{\text{lin–lin}}$	**0.316**	$\beta^L_{\text{lin–lin}}$
3	4.92	0.557	$\beta^L_{\text{lin–lin}}$	**0.472**	$\beta^L_{\text{lin–lin}}$

Boldface numbers show the minimum error values in each row.

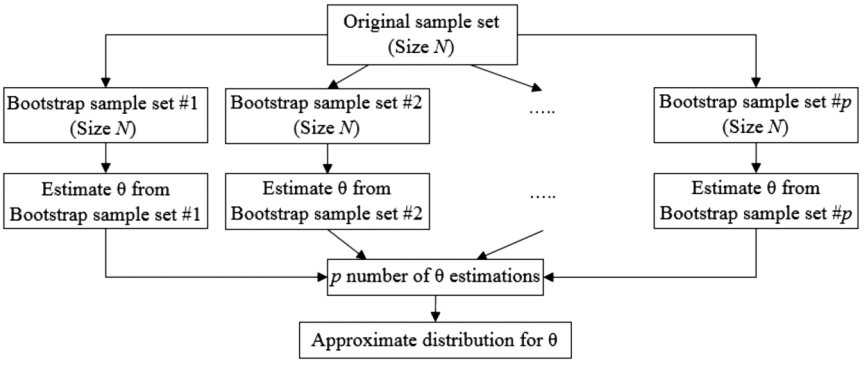

Fig. 7 The framework for the bootstrap method (see also Picheny et al. [24]).

Table 14 Comparison of the confidence interval for MCMC-TM and the RMSE of MCMC-TM for all problems

Problem ID	n_{var}	Rel. index, β	Mean, median predictions for MCMC-TM	95% Confidence intervals	Confidence interval divided by 4	RMSE for MCMC-TM
1	2	3.00	3.189, 3.185	2.770–3.645	0.219	0.225
		4.00	4.003, 3.993	3.409–4.673	0.316	0.344
		5.00	5.094, 5.049	4.225–6.098	0.468	0.473
2	2	3.03	2.812, 2.716	2.375–3.690	0.329	0.265
		4.00	4.221, 4.313	2.982–5.499	0.629	0.480
		5.00	4.984, 5.025	3.195–7.695	1.125	0.630
3	2	2.95	2.799, 2.777	2.389–3.325	0.234	0.211
		4.00	3.526, 3.470	3.058–4.320	0.316	0.395
		5.05	4.125, 4.077	3.447–5.364	0.479	0.532
4	2	3.03	2.900, 2.896	2.654–3.179	0.131	0.191
		3.42	3.534, 3.454	2.877–4.724	0.462	0.376
		4.46	3.940, 3.802	3.061–5.826	0.691	1.010
5	4	3.01	3.202, 3.184	2.738–3.735	0.249	0.241
		4.01	4.186, 4.162	3.446–5.038	0.398	0.369
		5.01	5.216, 5.195	4.223–6.390	0.542	0.512
6	6	3.06	2.981, 2.970	2.545–3.498	0.238	0.247
		4.05	3.918, 3.906	3.272–4.603	0.333	0.374
		5.08	4.956, 4.918	4.094–6.059	0.491	0.540
7	6	3.03	2.849, 2.802	2.487–3.408	0.230	0.259
		4.03	3.156, 3.029	2.470–4.521	0.513	0.547
		5.03	4.146, 3.844	3.004–6.606	0.901	0.948
8	6	3.00	2.787, 2.737	2.431–3.365	0.234	0.238
		4.02	3.610, 3.493	2.843–4.983	0.535	0.495
		5.04	4.314, 4.004	3.236–6.559	0.831	0.808
9	9	3.02	3.096, 3.073	2.623–3.760	0.284	0.271
		4.04	3.608, 3.387	2.746–5.778	0.758	0.553
		5.09	4.151, 3.717	3.054–7.238	1.046	0.950
10	12	3.05	2.894, 2.857	2.464–3.470	0.252	0.267
		4.02	3.538, 3.355	2.804–5.063	0.565	0.523
		5.07	4.585, 4.277	3.272–7.285	1.003	0.834
Wind turbine	4	3.69	3.677, 3.649	3.132–4.409	0.319	0.316
	3	4.92	4.837, 4.783	4.008–5.949	0.485	0.472

It must be noted that derivation of an analytical formula that could provide the confidence for a given number of samples would be appealing such that the number samples could be estimated for an estimated reliability and desired confidence level. However, as noted by Picheny et al. [24] it is not easy to derive such an analytical formula.

V. Conclusions

An efficient tail modeling method based on the use of Markov chain Monte Carlo (MCMC) method with Metropolis–Hastings algorithm was proposed in this paper. A commonly used proposal distribution formula was modified by using a scale parameter. The optimal value of this scale parameter was obtained for various numerical example problems with a varying number of random variables, and an approximate relationship was obtained between the optimal value of the scale parameter and the number of random variables. From the results obtained from these studies, the following were observed:

1) It is found that as the number of random variables in the problem increases, the optimum k value also increases. It is also observed that there is no clear correlation between the reliability level of the problem and the optimum k value.

2) The approximate relationship obtained between the optimal value of the proposal distribution scale parameter and the number of random variables was found to work well for the reliability prediction of a horizontal axis wind turbine.

In addition, the performance of the proposed method, named MCMC-TM, was compared with that of the classical tail modeling (CTM) for the numerical example problems as well as the reliability prediction of a horizontal axis wind turbine. From the findings of these investigations, the following were observed:

1) For the numerical example problems, MCMC-TM was more accurate than CTM when the number of variables is less than or equal to four. For six-variable problems, MCMC-TM was more accurate than CTM for six cases out of nine. For a larger number of random variables, it was observed that both approaches have similar accuracies.

2) For the wind turbine reliability estimation problem, MCMC-TM predictions were more accurate than CTM predictions.

Moreover, bootstrap method is used to compute the confidence intervals of the reliability estimations. It is observed that the confidence intervals computed through the bootstrap method have good agreement with the root mean square error values, which are unavailable for practical problems.

Furthermore, the dependency of the scale parameter k on the nature of the limit-state function (LSF) and the statistical properties of the LSF is analyzed. The linearity and the roughness of the LSF are used as measures of the nature of the LSF. The c.o.v., skewness, and kurtosis are used as key statistical properties of the limit state function. It is found that there is no linear relationship between these measures and the scale parameter k.

Finally, the dependency of the performance of the proposed method on the probability distribution types of the input random variables was explored. It is found that the performance of MCMC-TM is not dependent on the probability distribution types of the input random variables.

Appendix A: Definitions of the Numerical Example Problems

In this study, the LSF of the example problems are formulated such that the positive value of the LSF denotes failure, because the upper tail of the probability distribution is modeled. It must be noted that this formulation is opposed to the conventional LSF setting, where the negative value of the LSF designates failure.

For all numerical example problems, three different reliability levels are considered by changing a proper term in the LSF (see Table A1). For instance, for the simple example problem, three different μ_R terms are used (70, 60, and 50, respectively) to obtain three different reliability index values (3.0, 4.0, and 5.0, respectively). Similarly, for the Branin–Hoo example problem, three different y_{crit} terms are used (190, 380, and 850, respectively) to obtain three different reliability index values (3.03, 4.0, and 5.0, respectively). The reliability index values reported in Table A1 are predicted using crude Monte Carlo simulations with 10^9 samples.

Table A1 The reliability levels considered for the example problems

ID	Problem	Term[a]	Value[b]	β[c]	Value[b]	β[c]	Value[b]	β[c]
1	Simple example	μ_R	70	3.00	60	4.00	50	5.00
2	Branin–Hoo	y_{crit}	190	3.03	380	4.00	850	5.00
3	Camelback	y_{crit}	400	2.95	1400	4.00	5000	5.05
4	Tuned mass damper	y_{crit}	48	3.03	53	3.42	54	4.46
5	Central crack	K_{IC}	44	3.01	52	4.01	63	5.01
6	Rotating disk	y_{crit}	0.38	3.06	0.36	4.05	0.34	5.08
7	Rosenbrock (6 var.)	y_{crit}	1.7×10^6	3.03	3.4×10^6	4.03	6.3×10^6	5.03
8	Dixon–Price (6 var.)	y_{crit}	3.5×10^3	3.00	8.4×10^3	4.02	18×10^3	5.04
9	Rosenbrock (9 var.)	y_{crit}	2.0×10^6	3.02	3.8×10^6	4.04	7.0×10^6	5.09
10	Dixon–Price (12 var.)	y_{crit}	9×10^3	3.05	19×10^3	4.02	40×10^3	5.07

[a]The term in the LSF that is varied to change the reliability level.
[b]The value of the term.
[c]Corresponding reliability index.

A.1. Two-Variable Simple Example

This problem is a two-variable simple problem with a linear LSF given as

$$Y = R - C \tag{A1}$$

where R denotes the response (e.g., stress), C denotes the capacity (e.g., strength), and both are random variables. The statistical properties of these random variables are provided in Table A2. The mean value of the response μ_R is changed to obtain various levels of reliability index values. For this problem, the actual reliability index can be obtained easily from Eq. (A2) as the LSF is linear and both random variables follow normal distribution. In Eq. (A2), μ and σ correspond to the mean and standard deviation of the corresponding quantity.

$$\beta = \frac{\mu_C - \mu_R}{\sqrt{\sigma_C^2 + \sigma_R^2}} = \frac{100 - \mu_R}{\sqrt{8^2 + 6^2}} = 10 - \frac{\mu_R}{10} \tag{A2}$$

A.2. Branin–Hoo

Branin–Hoo function can be defined in terms of the random variables x_1 and x_2 as

$$y_{bh}(x_1, x_2) = \left(x_2 - \frac{5.1x_1^2}{4\pi^2} + \frac{5x_1}{\pi} - 6\right)^2 + 10\left(1 - \frac{1}{8\pi}\right)\cos(x_1) + 10 \tag{A3}$$

The LSF for this problem can be written as

$$Y = y_{bh}(x_1, x_2) - y_{crit} \tag{A4}$$

In this problem, the random variables x_1 and x_2 follow normal distributions. The mean values of x_1 and x_2 are taken as 2.5 and 7.5, respectively. The standard deviations of both x_1 and x_2 are taken as 2.5. The value of y_{crit} in Eq. (A4) is varied to adjust the reliability level (see Table A1). Branin–Hoo function is depicted in Fig. A1.

A.3. Camelback

Camelback function can be defined in terms of the random variables x_1 and x_2 as

$$y_{cam}(x_1, x_2) = \left(4 - 2.1x_1^2 + \frac{x_1^4}{3}\right)x_1^2 + x_1x_2 + \left(-4 + 4x_2^2\right)x_2^2 \tag{A5}$$

Table A2 Statistical properties of the random variables in the simple example problem

Random variable	Distribution	Mean	Standard deviation
R	Normal	μ_R	6
C	Normal	100	8

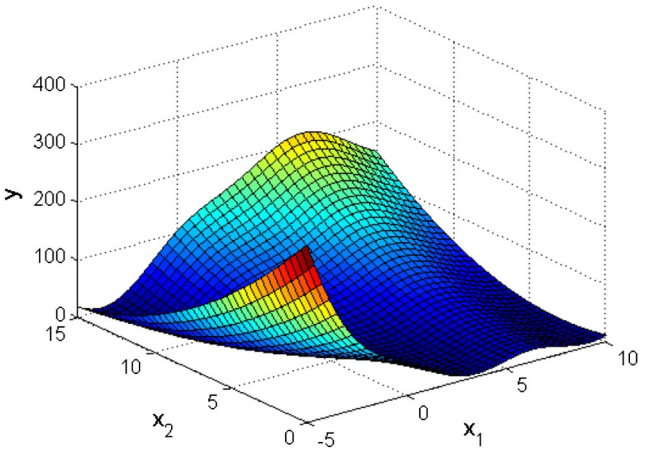

Fig. A1 Branin–Hoo function.

The LSF for this problem can be written as

$$Y = y_{cam}(x_1, x_2) - y_{crit} \tag{A6}$$

In this problem, the random variables x_1 and x_2 follow standard normal distributions. The value of y_{crit} in Eq. (A6) is varied to adjust the reliability level of this problem (see Table A1). Camelback function is depicted in Fig. A2.

A.4. Tuned Mass Damper

The tuned vibration absorber problem is a damped single–degree-of-freedom system with dynamic vibration absorber shown in

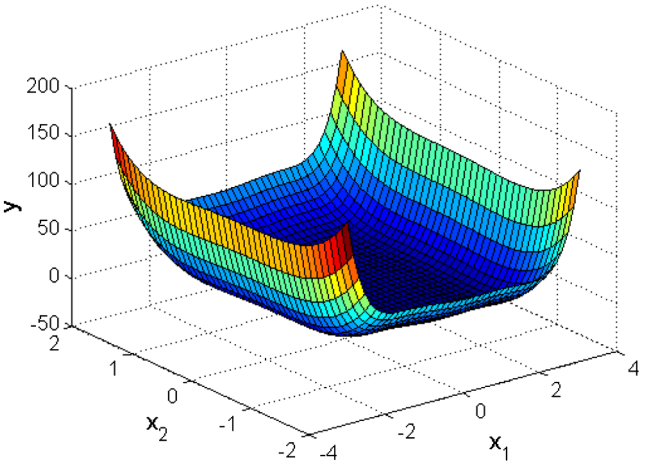

Fig. A2 Camelback function.

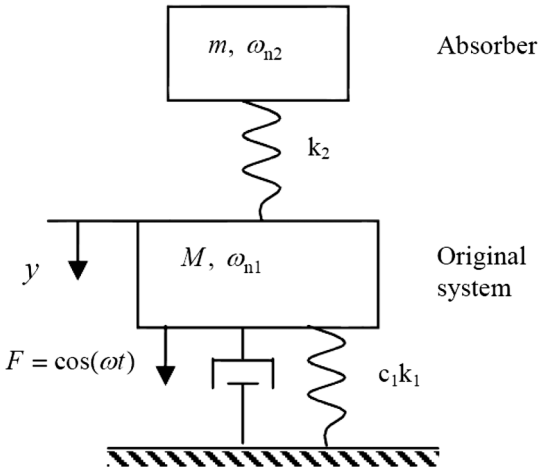

Fig. A3–1 Tuned vibration absorber.

Fig. A3–1. The original system is externally excited by a harmonic force and the vibration of the system is reduced by the absorber. The amplitude of the vibration depends on the following system parameters:

1) $R = m/M$, the mass ratio of the absorber to the original system
2) ζ, the damping ratio of the original system
3) $b_1 = \omega_{n1}/\omega$, the ratio of the natural frequency of the original system to the excitation frequency
4) $b_2 = \omega_{n2}/\omega$, the ratio of the natural frequency of the absorber to the excitation frequency

The LSF for this problem can be expressed as

$$Y = y_{\text{tmd}}(b_1, b_2) - y_{\text{crit}} \tag{A7}$$

where $y_{\text{tmd}}(b_1, b_2)$ is the amplitude of the system normalized by the amplitude of the quasi-static response of the system, and this normalized amplitude can be calculated from

$$y_{\text{tmd}}(b_1, b_2) = \frac{|1 - (1/b_2)^2|}{\sqrt{[1 - R(1/b_1)^2 - (1/b_1)^2 - (1/b_2)^2 + (1/b_1 b_2)^2]^2 + 4\zeta^2[(1/b_1) - (1/b_1 b_2^2)]^2}} \tag{A8}$$

The random variables of the problem are b_1 and b_2, and they follow normal distribution with a mean value of 1.0 and standard deviation of 0.025. R and ζ are taken as deterministic variables possessing the following values: $R = 0.01$ and $\zeta = 0.01$. The normalized amplitude of the original system is plotted in Fig. A3–2. The value of y_{crit} in Eq. (A7) can be adjusted to obtain various values of reliability indices given in Table A1.

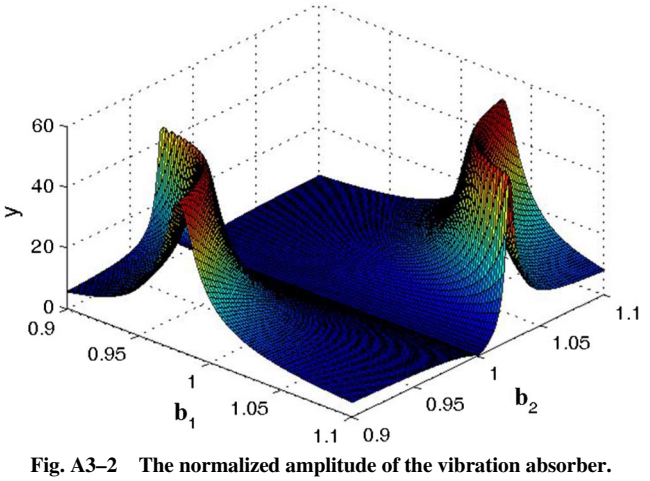

Fig. A3–2 The normalized amplitude of the vibration absorber.

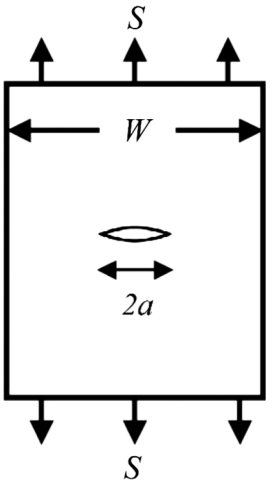

Fig. A4 Central cracked plate with a finite width.

A.5. Central Crack

In this example problem, a rectangular plate of finite width W having a central through-thickness crack of length $2a$ loaded in tension with a uniform stress, S, is considered (see Fig. A4). The LSF for this problem can be written as

$$Y = \sqrt{\sec\left(\frac{\pi a}{W}\right)} S\sqrt{\pi a} - K_{\text{IC}} \tag{A9}$$

where a is the half crack length, W is the plate width, S is the applied stress, K_{IC} is the fracture toughness, and all these variables are taken random. The probability distributions and the mean and the standard deviations of the random variables are given in Table A3. The mean value of the fracture toughness ($\bar{K}_{\text{IC}}$) is varied to adjust the reliability level of the problem (see Table A1).

A.6. Rotating Disk

This example problem is taken from Penmetsa and Grandhi [27]. The burst margin (M_b) of a rotating disk (see Fig. A5) is defined as the margin of safety before an overstress condition occurs due to the stress on the part being too large for the material to withstand. The LSF for this problem is defined such that the burst margin should not be smaller than a critical value, y_{crit}.

$$Y = M_b - y_{\text{crit}}; \quad M_b = \sqrt{\alpha_m S_U \Big/ \left[\frac{\rho(2\pi\omega)^2(R_o^3 - R_i^3)}{3(385.82)(R_o - R_i)}\right]} \tag{A10}$$

where α_m is the material utilization factor (a safety factor) to account for uncertainties and unknown material properties, S_U is the ultimate tensile strength, ρ is the density, ω is the rotational speed, and R_o and R_i are the outer and inner radii of the disk. The statistical properties of

Table A3 Statistical properties of the random variables

Random variable	Distribution	Mean	Standard deviation
a, mm	Normal	25	0.75
W, mm	Normal	500	5
S, MPa	Normal	100	100
K_{IC}, MPa$\sqrt{m}$	Normal	$\bar{K}_{\text{IC}}$	0.1 $\bar{K}_{\text{IC}}$

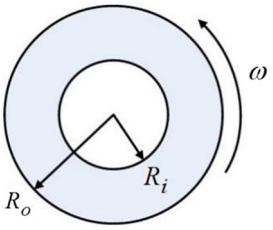

Fig. A5 The geometry of the rotating disk.

Table A4 Statistical properties of the random variables in the rotating disk problem

Random variable	Distribution	Mean	Standard deviation
α_m	Normal	0.9377	0.0459
S_U, $1b/in^2$	Normal	220,000	5,000
ω, rpm	Normal	21,000	1,000
ρ, $1b/in^3$	Normal	0.29	0.0058
R_o, in	Normal	24	0.5
R_i, in	Normal	8	0.3

the random variables in this problem are given in Table A4. The value of y_{crit} in Eq. (A10) is changed to obtain various reliability index values (see Table A1).

A.7. Rosenbrock: 6-Variable Case

Rosenbrock function can be defined in terms of the random variable vector $\boldsymbol{x}$ as

$$y_{rb}(\boldsymbol{x}) = \sum_{i=1}^{m-1}[(1-x_i)^2 + 100(x_{i+1}-x_i)^2] \tag{A11}$$

In the 6 variable case of this problem, $m = 6$ is used. The LSF for this problem can be written as

$$Y = y_{rb}(x_1, x_2) - y_{crit} \tag{A12}$$

In this problem, all random variables follow normal distributions. The mean values of the random variables are all taken as 2.5. The standard deviations of the random variables are all taken as 2.5. The value of y_{crit} in Eq. (A12) is varied to adjust the reliability level of this problem (see Table A1).

A.8. Dixon–Price: 6-Variable Case

Dixon–Price function can be defined in terms of the random variable vector $\boldsymbol{x}$ as

$$y_{dp}(\boldsymbol{x}) = (x_1-1)^2 + \sum_{i=2}^{m} m(2x_i^2 - x_{i-1})^2 \tag{A13}$$

In the 6-variable case of this problem, $m = 6$ is used. The LSF for this problem can be written as

$$Y = y_{dp}(x_1, x_2) - y_{crit} \tag{A14}$$

In this problem, all random variables follow standard normal distributions. The value of y_{crit} in Eq. (A14) is varied to adjust the reliability level of this problem (see Table A1).

A.9. Rosenbrock: 9-Variable Case

In the 9-variable case of the Rosenbrock problem, $m = 9$ is used. The value of y_{crit} in Eq. (A12) is varied to adjust the reliability level of the problem.

A.10. Dixon–Price: 12-Variable Case

In the 12-variable case of the Dixon–Price problem, $m = 12$ is used. The value of y_{crit} in Eq. (A14) is varied to adjust the reliability level of the problem.

Appendix B: Dependency of the Scale Parameter on the Nature and the Statistical Properties of the Limit State Function

In this section, the dependency of the scale parameter k on the nature and the statistical properties of the LSF is investigated. The linearity and the roughness of the LSF are used as measures of the nature of the LSF. The linearity of the LSF is assessed by computing the coefficient of determination (R^2) of the linear response surface constructed in the range of mean plus/minus three times the standard deviation of the input random variables. The linear response surfaces are constructed by generating 100,000 data points in the input random variable range mentioned above. The roughness of the limit state function is computed using Eq. (B1), which is derived from the bending energy functional [28,29]

$$\text{roughness} = \int_{\Omega} \sum_{i=1}^{n_{var}} \sum_{j=1}^{n_{var}} \left(\frac{\partial^2 y}{\partial x_i \partial x_j}\right)^2 d\boldsymbol{x} \tag{B1}$$

where Ω is the domain of input random variables. This integral is computed in the range of mean plus/minus three times the standard deviation of the input random variables through Monte Carlo integration using 100,000 samples. In this study, we use a nondimensional measure of roughness by normalizing the input variables ($\boldsymbol{x}$) as well as the output variable (y) to [0, 1].

The coefficient of variation (c.o.v.), skewness, and kurtosis are used as key statistical properties of the limit state function. These properties are computed by using crude MCS with sample size of 10^8.

Table B1 shows the variation of the scale parameter k with respect to the R^2, roughness, coefficient of variation, skewness, and kurtosis

Table B1 Dependency of the scale parameter with respect to the nature and the statistical properties of the limit state function

ID	Problem	k^*	R^2	Roughness	c.o.v.	Skewness	Kurtosis
1	Simple example	0.5661	1.0	0	0.250	0	3
2	Branin–Hoo	0.6336	0.145	1.07E + 06	0.084	1.853	9.901
3	Camelback	0.5348	2.7×10^{-4}	1.95E + 09	0.028	13.99	526.2
4	Tuned mass damper	0.4527	0.004	93.9	0.108	4.074	27.49
5	Central crack	0.6699	0.999	8.91E − 02	0.249	0.002	3
6	Rotating disk	0.7151	0.993	1.03E − 07	0.286	−0.2473	3.129
7	Rosenbrock (6 var.)	0.8825	0.477	1.90E + 06	0.064	3.344	23.72
8	Dixon–Price (6 var.)	0.8575	0.051	1.37E + 05	0.047	4.984	55.13
9	Rosenbrock (9 var.)	0.9157	0.471	1.91E + 06	0.074	2.656	16.21
10	Dixon–Price (12 var.)	0.9322	0.052	1.45E + 05	0.058	3.566	29.51

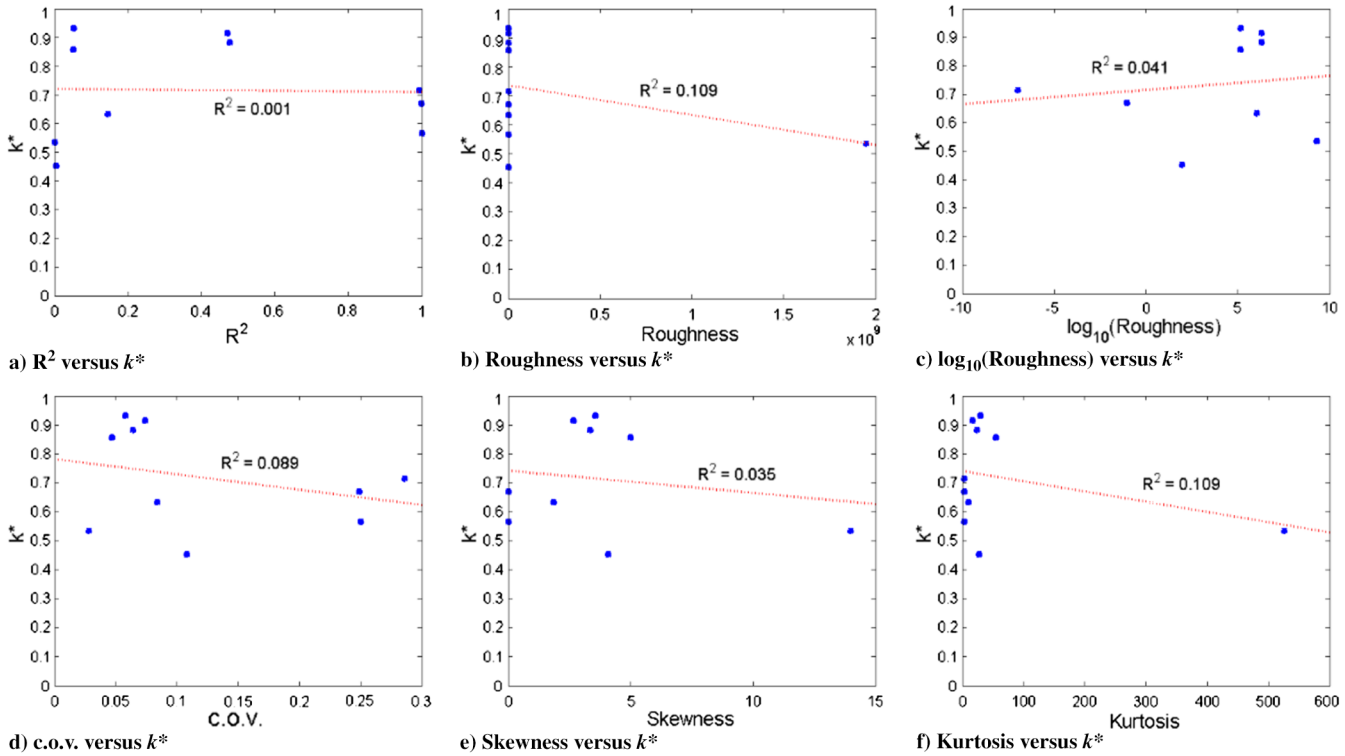

a) R^2 versus k^* b) Roughness versus k^* c) $\log_{10}$(Roughness) versus k^*

d) c.o.v. versus k^* e) Skewness versus k^* f) Kurtosis versus k^*

Fig. B1 Variation of the scale parameter with respect to the nature and the statistical properties of the limit state function.

of the limit state function. These variations are graphically depicted in Fig. B1. It is observed that there is no linear relationship between these measures and the scale parameter k (notice the small R^2 values given in the figures).

Appendix C: Dependency of the Performance of the Proposed Method on the Probability Distribution Types of the Input Random Variables

In this section, the dependency of the performance of the proposed method on the probability distribution types of the input random variables is explored. From the 10 example problems considered, 3 of them (namely, the 2-variable simple example problem, 6-variable Dixon–Price problem, and 12-variable Dixon–Price problem) are selected as representative problems for this investigation. The reasons for selecting these particular example problems are twofold: 1) the number of input random variables is represented well; 2) MCMC-TM has good performance over CTM for these problems.

The investigation in Sec. IV considered normally distributed input normal variables; however, the performances of tail modeling techniques (CTM, MCMC-TM, or other tail modeling methods) are not dependent on the distribution type of the input random variables. Therefore, distribution types other than normal distribution are also considered. Normal and lognormal distributions are used in the simple example problem. Normal, lognormal, and uniform distributions are used in the six-variable Dixon–Price problem. Normal, lognormal, uniform, and Weibull distributions are used in the 12-variable Dixon–Price problem. The modified statistical properties of the random variables in these example problems are given in Tables C1–C3. As the lognormal distribution does not allow negative values, we changed the mean values of the input variables from 0 to 10.

Table C1 Modified statistical properties of the random variables in the simple example problem

Random variable	Distribution	Mean	Standard deviation
R	Normal	μ_R	6
C	Lognormal	100	8

The numerical procedure outlined in Sec. IV is applied, and the optimal values of the scale parameter k as well as the prediction errors (RMSE) of the CTM and MCMC-TM are computed. Table C4 represents the optimum k values for the selected example problems. Comparing the optimum k values in Table C4 to those in Table 7, it is seen that the optimum k values in both tables are close.

Table C5 provides comparison of the RMSE of CTM and MCMC-TM for the selected examples. It is observed that MCMC-TM has smaller RMSE values than CTM for the three selected problems for

Table C2 Modified statistical properties of the random variables in the six-variable Dixon–Price problem

Random variable	Distribution	Mean	Standard deviation
x_1, x_2	Normal	10	1
x_3, x_4	Lognormal	10	1
x_5, x_6	Uniform	10	1

Table C3 Modified statistical properties of the random variables in the 12-variable Dixon–Price problem

Random variable	Distribution	Mean	Standard deviation
x_1, x_2, x_3	Normal	10	1
x_4, x_5, x_6	Lognormal	10	1
x_7, x_8, x_9	Uniform	10	1
x_{10}, x_{11}, x_{12}	Weibull	10	1

Table C4 Optimum k values for the selected example problems

ID	Problem	n_{var}	For β_{low}	For β_{med}	For β_{high}	Average
1	Simple example	2	0.4977	0.5099	0.5569	0.5215
8	Dixon–Price (6 var.)	6	0.5501	0.8009	0.8351	0.7287
10	Dixon–Price (12 var.)	12	0.7501	0.8218	0.9110	0.8276

Table C5 Comparison of the RMSE of CTM and MCMC-TM for the selected examples

Problem ID	n_{var}	LSF term	Rel. index, β	RMSE for CTM	RMSE for MCMC-TM
1	2	$\mu_R = 71$	3.06	0.245	**0.220**
		$\mu_R = 62$	4.07	0.403	**0.321**
		$\mu_R = 54$	5.02	0.581	**0.439**
8	6	$y_{\text{crit}} = 1270$	3.03	0.364	**0.299**
		$y_{\text{crit}} = 1500$	4.01	0.719	**0.595**
		$y_{\text{crit}} = 1850$	5.04	1.027	**0.997**
10	12	$y_{\text{crit}} = 4.13 \times 10^6$	2.98	0.368	**0.315**
		$y_{\text{crit}} = 4.56 \times 10^6$	4.00	0.862	**0.689**
		$y_{\text{crit}} = 5.06 \times 10^6$	5.04	1.389	**1.116**

Boldface numbers show the minimum error values in each row.

all reliability levels. These results show that the performance of MCMC-TM is not dependent on the probability distribution types of the input random variables, a good property possessed by tail modeling methods.

Acknowledgments

The authors gratefully acknowledge the support provided by The Scientific and Technological Research Council of Turkey (TÜBİTAK), under award MAG-214M205. The authors thank Prof. Palani Ramu at the Indian Institute of Technology Madras and Ms. Nahide Tüten at the TOBB University of Economics and Technology for their helpful comments.

References

[1] Liu, J. S., *Monte Carlo Strategies in Scientific Computing*, Springer–Verlag, New York, 2001.

[2] Melchers, R. E., "Importance Sampling in Structural Systems," *Structural Safety*, Vol. 6, No. 1, 1989, pp. 3–10. doi:10.1016/0167-4730(89)90003-9

[3] Wu, Y. T., "Computational Methods for Efficient Structural Reliability and Reliability Sensitivity Analysis," *AIAA Journal*, Vol. 32, No. 8, 1994, pp. 1717–1723. doi:10.2514/3.12164

[4] Nie, J., and Ellingwood, B. R., "Directional Methods for Structural Reliability Analysis," *Structural Safety*, Vol. 22, No. 3, 2000, pp. 233–249. doi:10.1016/S0167-4730(00)00014-X

[5] Boos, D., "Using Extreme Value Theory to Estimate Large Percentiles," *Technometrics*, Vol. 26, No. 1, 1984, pp. 33–39. doi:10.1080/00401706.1984.10487919

[6] Hasofer, A., "Non-Parametric Estimation of Failure Probabilities," *Mathematical Models for Structural Reliability*, edited by F. Casciati, and B. Roberts, CRC Press, Boca Raton, FL, 1996, pp. 195–226.

[7] Caers, J., and Maes, M., "Identifying Tails, Bounds, and End-Points of Random Variables," *Structural Safety*, Vol. 20, No. 1, 1998, pp. 1–23. doi:10.1016/S0167-4730(97)00036-2

[8] Ramu, P., Kim, N.-H., and Haftka, R. T., "Multiple Tail Median Approach for High Reliability Estimation," *Structural Safety*, Vol. 32, No. 2, 2010, pp. 124–137. doi:10.1016/j.strusafe.2009.09.002

[9] Acar, E., "Guided Tail Modeling for Efficient and Accurate Reliability Estimation of Highly Safe Mechanical Systems," *Proceedings of the Institution of Mechanical Engineers Part C: Journal of Mechanical Engineering Science*, Vol. 225, No. 5, 2011, pp. 1237–1251.

[10] Acar, E., "Reliability Prediction Through Guided Tail Modeling Using Support Vector Machines," *Proceedings of the Institution of Mechanical Engineers Part C: Journal of Mechanical Engineering Science*, Vol. 227, No. 12, 2013, pp. 2780–2794.

[11] Ramu, P., and Krishna, M., "A Variable-Fidelity and Convex Hull Approach for Reliability Estimates in Tail Modeling," *14th AIAA/ISSMO Multidisciplinary Analysis and Optimization Conference*, AIAA Paper 2012-5628, Sept. 2012.

[12] Rahman, S., and Xu, H., "A Univariate Dimension Reduction Method for Multi-Dimensional Integration in Stochastic Mechanics," *Probabitistic Engineering Mechanics*, Vol. 19, No. 4, 2004, pp. 393–408. doi:10.1016/j.probengmech.2004.04.003

[13] Karian, Z. E., Dudewicz, E. J., and McDonald, P., "The Extended Generalized Lambda Distribution System for Fitting Distributions to Data: History, Completion of Theory, Tables, Applications, the "Final Word" on Moment Fits," *Communication in Statistics—Simulation and Computation*, Vol. 25, No. 3, 1996, pp. 611–642. doi:10.1080/03610919608813333

[14] Hosking, J. R. M., and Wallis, J. R., "Parameter and Quantile Estimation for the Generalized Pareto Distribution," *Technometrics*, Vol. 29, No. 3, 1987, pp. 339–349. doi:10.1080/00401706.1987.10488243

[15] Muraleedharan, G., Soares, C. G., and Lucas, C., "Characteristic and Moment Generating Functions of Generalised Extreme Value Distribution (GEV)," *Sea Level Rise, Coastal Engineering, Shorelines and Tides*, edited by L. L. Wright, Nova Science Publ., New York, 2011, pp. 269–276.

[16] Ditlevsen, O., "Generalized Second Moment Reliability Index," *Journal of Structural Mechanics*, Vol. 7, No. 4, 1979, pp. 435–451. doi:10.1080/03601217908905328

[17] Hastings, W. K., "Monte Carlo Sampling Methods Using Markov Chains and Their Applications," *Biometrika*, Vol. 57, No. 1, 1970, pp. 97–109. doi:10.1093/biomet/57.1.97

[18] Gilks, W. R., Richardson, S., and Spiegelhalter, D. J., *Markov Chain Monte Carlo in Practice*, Chapman and Hall, London, 1996.

[19] Au, S. K., and Beck, J. L., "A New Adaptive Importance Sampling Scheme for Reliability Calculations," *Structural Safety*, Vol. 21, No. 2, 1999, pp. 135–158. doi:10.1016/S0167-4730(99)00014-4

[20] Rosenthal, J. S., "Optimal Proposal Distributions and Adaptive MCMC," *Handbook of Markov Chain Monte Carlo*, 1 S. Brooks, A. Gelman, G. L. Jones, and X.-L. Meng, Chapman & Hall/CRC, Boca Raton, 2011, Chap. 4.

[21] Ceyhan, O., Ortakaya, Y., Korkem, B., Sezer-Uzol, N., and Tuncer, I. H., "Optimization of Horizontal Axis Wind Turbines by Using BEM Theory and Genetic Algorithm," *5th Ankara International Aerospace Conference*, Middle East Technical Univ., AIAC Paper 2009-044, Ankara, 2009.

[22] Burton, T., Sharpe, D., Jenkins, N., and Bossanyi, E., *Wind Energy Handbook*, Wiley, New York, 2001.

[23] Snel, H., "Review of Aerodynamics for Wind Turbines," *Wind Energy*, Vol. 6, No. 3, 2003, pp. 203–211. doi:10.1002/(ISSN)1099-1824

[24] Picheny, V., Kim, N.-H., and Haftka, R. T., "Application of Bootstrap Method in Conservative Estimation of Reliability with Limited Samples," *Structural and Multidisciplinary Optimization*, Vol. 41, No. 2, 2010, pp. 205–217. doi:10.1007/s00158-009-0419-8

[25] Chernick, M. R., *Bootstrap Methods, A Guide for Practitioners and Researchers*, 2nd ed., Wiley Series in Probability and Statistics, Wiley, Hobeken, NJ, 2008.

[26] Efron, B., *The Jackknife, the Bootstrap and Other Resampling Plans*, CBMS-NSF Regional Conference Series in Applied Mathematics, SIAM, Philadelphia, 1982.

[27] Penmetsa, R. C., and Grandhi, R. V., "Adaptation of Fast Fourier Transformations to Estimate Structural Failure Probability," *Finite Elements in Analysis and Design*, Vol. 39, Nos. 5–6, 2003, pp. 473–485. doi:10.1016/S0168-874X(02)00104-X

[28] Duchon, J., "Splines Minimizing Rotation-Invariant Semi-Norms in Sobolev Spaces," *Constructive Theory of Functions of Several Variables*, Springer, New York, 1977, pp. 85–100.

[29] Salem, M. B., and Tomaso, L., "Automatic Selection for General Surrogate Models," *12th World Congress of Structural and Multidisciplinary Optimisation*, International Soc. for Structural and Multidisciplinary Optimization, Braunschweig, Germany, June 2017, Paper 331.

R. K. Kapania
Associate Editor